Studying the Effects of Wall-Thickness and Diameter on the Mechanical Properties of SWNTS

A.R. Setoodeh[1], S. Safarian[2]
[1]*Department of Mechanical Engineering, Faculty of Engineering, Ferdowsi University of Mashhad, Mashhad 91775, Iran*

E-mail: setoodeh@um.ac.ir

[2] *Department of Mechanical Engineering, Faculty of Engineering, Azad University of Mashhad, Mashhad, Iran*

E-mail: safaryan_sobhan@yahoo.com

Abstract

An energy-equivalent model is employed to develop the mechanical properties of singled-walled carbon nanotube (SWCNTs). This method is based on the equivalence of both the system potential energy as well as the strain energy of SWCNT. In fact, the energy-equivalent model is a link between molecular mechanics and continuum mechanics. In this research, Young's and shear modulus as well as Poisson's ratio are obtained for both armchair and zigzag SWCNTs. The effects of nanotube diameter and wall-thickness are investigated on the mechanical behavior of these types of nanotubes. It is seen that Young's and shear modulus decrease significantly as the thickness of the SWCNT increases. Furthermore, elastic moduli of both armchair and zigzag carbon nanotubes increase monotonically and approach elastic moduli of graphite when the tube diameter is increased but the variation of Poisson's ratio is vice versa. Also, the stress-strain curve for the armchair SWCNT predicted. The results show that armchair nanotube exhibit slightly higher values of Young's modulus than zigzag ones for small values of radius, but their shear modulus are identical based on the present study. The developed results from a very simple approach, exhibit good agreement with the available solutions in the literature.

I. INTRODUCTION

In the past decade, significant progress has been achieved in the area of nano-engineering. Nano-structured materials have generated considerable interest in the materials research community in the last few years partly due to their potentially remarkable mechanical properties [1]. In particular, materials such as carbon nanotubes, nanowire, nanoparticle-reinforced polymers and metals, and nano-layered materials have shown considerable promise. For example, Carbon nanotubes that were discovered by Ijima (1991), could potentially have a Young's modulus as high as 1 TPa and a tensile strength approaching 100 GPa , about a hundred times higher than steel and can tolerate large strains (about 50%) before mechanical failure. The design and fabrication of these materials are performed on the nanometer scale with the ultimate goal to obtain highly desirable macroscopic properties. [2].

Until recently, nanostructures were modeled using molecular and quantum mechanics. On the other hand, structural mechanics was mostly used to study the behavior of macro-structures. As the top-to-bottom approach of modeling components is getting close to the micro-meter and nano-meter levels, issues on how to bridge the fields of molecular and structural mechanics are starting to emerge. One of these issues is the procedure of implementing structural stiffnesses for modeling nanostructures, such as carbon nanotubes.

The deformation behavior of CNTs has been the subject of numerous experimental, molecular dynamics (MD), and elastic continuum modeling studies. Experiments at this length scale are still under development and thus have resulted in a range of reported values for various mechanical properties. Furthermore, consistent interpretation of tube geometry when reducing data to properties remains an important issue. Spectroscopy, micrography and MD simulations have accurately mapped out the structure of CNTs. MD methods have also been effective in simulating the deformation of CNTs in tension, bending and torsion. However, the computational expense of MD simulations limits the size of the CNTs that can be studied using this technique. Despite the robustness of continuum mechanics, elastic models cannot be easily applied to CNTs, due to the presence of the inter-layer van der Waals forces and of dimensional and material property ambiguities associated with the single atomic layer thickness of the walls.

Zhang et al. [3, 4] proposed a nanoscale continuum theory, where the continuum strain energy density is evaluated by the bond energy on the atomic level for all atomic bonds in the cell, using the Cauchy-Born rule. The theory was first used to study the elastic modulus of a SWNT and then applied to the study of fracture nucleation in SWNTs under tension. In an alternative continuum approach, a representative volume element (RVE) of the chemical structure of graphene has been substituted with equivalent-truss and equivalent continuum models. Li and Chou [5] represented the chemical bond between items using a structural mechanics approach and by combining molecular and beam theory. They showed that mechanical behavior of armchair and zigzag SWCNTs depend strongly on tube diameter and weakly on chirality. Tserpes and Papanikos [6] proposed a three-dimensional finite element model for armchair, zigzag and chiral single walled carbon nanotubes, which was based on the assumption that the SWCNTs under loading behave like a beamed structure. They concluded that Young's modulus varies from 0.952 to 1.066 TPa and the shear modulus ranged from 0.242 to 0.504 TPa for a wall thickness equal to 0.34. Giannopoulos et al. [7] developed a non-continuum finite element method in order to compute the mechanical response of armchair and zigzag SWCNTs. The interatomic interactions were modeled using linear elastic spring elements instead of beam elements proposed by Li and Chou [5]. Most recently, an analytical molecular mechanics model proposed by Chang and Gao [8] to relate the elastic properties of a single-walled carbon nanotube to its atomic structure with calibrated force field constants. The developed analytical molecular mechanics model extended by Xiao et al. [9] to incorporate the modified Morse potential function to estimate elastic constants and stress–strain relationships of nanotubes under tensile and torsion loadings.

Wu et al. [10] put forward an energy-equivalent model for studying the mechanical properties of SWCNTs based on the link between molecular mechanics and solid mechanics.

Recently, Wu et al. [10] presented an energy-equivalent approach for modeling the deformation of SWCNTs. In their approach, they considered SWCNT as a thin cylinder subjected to an axial tension loading or torsion loading. For modeling SWCNTs with an energy-equivalent model, the authors used both the principle of molecular mechanics, and the total system potential energy associated with stretching and angle variation.

In this paper, by incorporating an energy-equivalent method we are able to predict the mechanical properties of SWCNTs not only in axial direction but also in hoop direction. Also, in-plane properties and stress–strain relationships of nanotubes under tensile loadings can be estimated easily. The energy-equivalent model is originated from Wu et al. [10] and is extended to model the behavior of carbon nanotubes under radial pressure. The present model includes the basic molecular structure, system potential energy, elastic behavior in the hoop direction, relationship between in-plane properties (both the Poisson's ratio and the surface Young's modulus) in hoop direction and those in axial direction.

II. THE MODEL OF MOLECULAR MECHANICS

There are several ways to view a SWCNT. The most widely used is by reference to rolling up graphene sheet to form a hollow cylinder with end caps. The cylinder is composed of hexagonal carbon rings, with the end caps of pentagonal rings. The hexagonal pattern is repeated periodically leading to binding of each carbon atom to three neighboring atoms with covalent bonds. This covalent bond is a very strong chemical bond and plays significant role to the impressive mechanical properties of graphitic and as a consequence, of all carbon-related nano-structures. The atomic structure of nanotubes depends on tube chirality, which is defined by the chiral vector C_h and the chiral angle θ. The chiral vector is defined as the line connected from two crystallographically equivalently sites O and C on a two-dimensional

graphene structure, as may be seen in Fig. 1. The chiral vector C_h can be defined in terms of the lattice translation indices (n, m) and the basic vectors a_1 and a_2 of the hexagonal lattice (see Fig. 1.) as follows,

$$\vec{C}_h = n\vec{a}_1 + m\vec{a}_2 \quad (1)$$

The chiral angle θ is the angle between the chiral vector C_h with respect to the zigzag direction (n, 0) where θ=0° and the unit vectors a_1 and a_2. For the chiral angles of 0° and 30°, the zigzag and armchair nanotubes are formed, respectively.

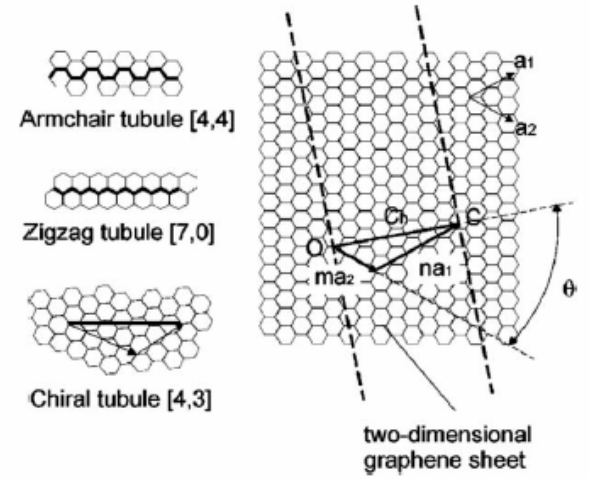

Figure1. Schematic of the hexagonal lattice of graphene sheet including definition of basic structural parameters and explanation of SWCNTs formation,

These two types of nanotubes correspond to the two limiting cases. In terms of the roll-up vector, the armchair nanotubes are defined by (n, n) and the zigzag nanotubes by (n, 0). For chiral angles different than 0° and 30°, the chiral nanotubes, which are defined by a pair of indices (n, m) with $n \neq m$, are formed. The integers (n**,** m) uniquely determine R and θ. The length L of the chiral vector C_h is directly related to the tube radius. The relationship between the integers (n, m) and the radius is given by *IIJIMA*. [11],

$$R = \ell_o \sqrt{3(n^2 + m^2 + nm)} / 2\pi \quad (2)$$

where ℓ_o is the length of the C–C bond which is 1.42Å. From the viewpoint of molecular mechanics, a carbon nanotube can be regarded as a large molecule consisting of carbon atoms. The atomic nuclei can be regarded as material points. Their motions are regulated by a force field, which is generated by electron–nucleus interactions and nucleus–nucleus interactions. Usually, the force field is expressed in the form of steric potential energy. It depends solely on the relative positions of the nuclei constituting the molecule. The general expression of the total steric potential energy, omitting the electrostatic interaction, is a sum of energies due to valence or bonded interactions and non-bonded interactions as,

$$U = U_\rho + U_\theta + U_\varphi + U_\omega + U_{vd\omega} \quad (3)$$

where Uρ is for a bond stretch interaction, U_θ for a bond angle bending, Uφ for a dihedral angle torsion, Uω for an improper (out-of-plane) torsion, Uvdω for a nonbonded van der Waals interaction, as shown in Fig. 2.

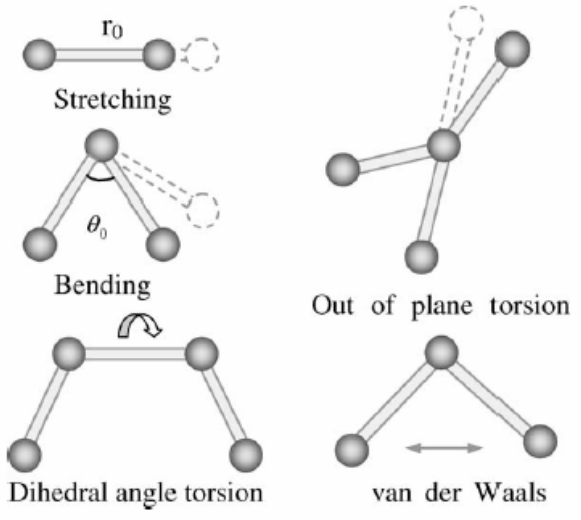

Figure2. Interatomic interactions in molecular mechanics.

For a SWCNT subjected to tension and torsion loadings, only bond stretching and angle variation terms are significant in the total system potential energy. Therefore, Eq. (3) can be simplified as,

$$U = U_\rho + U_\theta = \frac{1}{2}\sum_i K_i (dR_i)^2 + \frac{1}{2}\sum_j C_j (d\theta_j)^2 \quad (4)$$

where K_i and C_j are constants with respect to stretching and angle variance, respectively. dR_i and $d\theta_j$ are the elongations of bond i and the variance of bond angle j. Thus we can obtain the stretching force and the twisting moment equilibrium equations,

$$F = KdR, \quad M = Cd\theta \quad (5)$$

III. HOOP PROPERTIES OF SINGLE-WALLED NANOTUBES

The stiffness in the hoop direction of nanotubes (surface Young's modulus E_Θ) plays an important role in resisting deformation due to external radial pressure. Single-walled nanotubes subjected to hoop

force, which in turn is induced by radial pressure is studied in this section.

The idea of using an energy-equivalent model to studying the mechanical properties of single-walled carbon nanotubes (SWCNTs) is applied. The equivalent Young's modulus in the hoop direction of nanotubes for both armchair and zigzag SWCNTs are derived by combining the methods of molecular mechanics and continuum mechanics. At first, based on the principle of molecular mechanics, the total system potential energy associated with both stretching and angular variations is obtained. On the other hand, considering SWCNT as a thin cylinder subjected to a radial pressure, the strain energy can be obtained based on continuum mechanics. Here, we modify the effective energy-equivalent system to model the in-plane properties of nanotubes under hoop compression (no axial pressure is applied).

A. An armchair nanotube

An armchair nanotube (n = m) subjected to hoop force resultant is studied first. Fig. 3. shows an equilibrium configuration of the tube and the associated forces and moments in three chemical bonds *a*, *b*, *b*, three bond angles α, β, β resulting from two bond elongation *da* and *db* and two bond angle variances $d\alpha$ and $d\beta$. The relationship between hoop force resultant, the bond stretch and bond angle variation can be determined through equilibrium and geometry of the nanotube structure. It is noticed that the armchair molecular structure under compression along the hoop direction is similar to the zigzag configuration under axial compression. The following analysis will determine if the armchair hoop direction is equivalent to the zigzag structure.

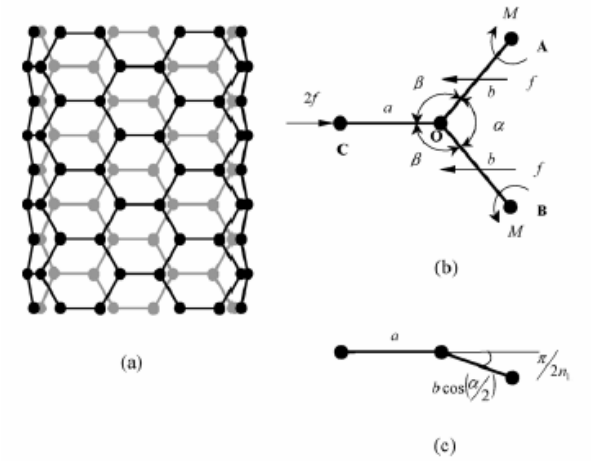

Figure3. Schematic illustration of (a) an armchair carbon nanotube, (b) analytical model for hoop compression, and (c) geometry relationship.

An armchair nanotube subjected to a radial pressure is considered first. According to its structure and deformation characters, the carbon–carbon bond and the bond angle can be classified into two types of bonds and bond angles. They are called bonds *a* and *b*, and angles α and β, respectively as shown in Fig. 3(b). We assume that the force exerted on bond *b* in the hoop direction is denoted by *f*. Using the force equilibrium of bond extension, the bond elongation *da* and *db* would be,

$$da = \frac{2f}{K} \tag{6}$$

$$db = \frac{f\cos(\alpha/2)}{K} \tag{7}$$

where *da* and *db* are the bond elongations of bond *a* and bond *b*. We take the relation $a = b = \ell_o$ in the undeformed configuration. Letting $\alpha = 120^\circ$, the bond stretching potential energies of an armchair nanotube are obtained,

$$\begin{aligned} U\rho a &= \frac{1}{2}K(da)^2 = \frac{2f^2}{K} \\ U\rho b &= \frac{1}{2}K(db)^2 = \frac{f^2}{8K} \end{aligned} \tag{8}$$

The expressions of the bond angle variations $d\alpha$ and $d\beta$ must be found first in order to obtain the energy. For convenience, bond *b* is divided into two halves, so the rotation moment exerted on the right half in plane b–b would be equal to $f\ell_o\sin(\alpha/2)/2$. On the other hand, rotation moment produced by the bond angle $d\alpha$ in plane b–b is $Cd\alpha$, and similary in plane a–b is $Cd\beta$. Thus the moment equilibrium equation can be written as,

$$f(\frac{\ell_o}{2})\sin(\alpha/2) = Cd\alpha + Cd\beta\cos\varphi \tag{9}$$

where φ is the torsion angle between plane b–b and plane a–b, which can be calculated by,

$$\cos\varphi = \frac{\tan(\alpha/2)}{\tan\beta} \tag{10}$$

and for the armchair nanotube, the geometry relationships satisfy,

$$\cos\beta = \cos(\alpha/2)\cos(\pi - \frac{\pi}{2n}) \tag{11}$$

where $(\pi - \frac{\pi}{2n})$ is the angle of the bond OC to the plane OA–OB as shown in Fig. 3c.
Differentiating Eq. (11), one has,

$$d\beta = -\frac{\sin(\alpha/2)}{2\sin\beta}\cos(\frac{\pi}{2n})d\alpha \tag{12}$$

Substituting Eq. (12) into Eq. (9), the expression of $d\alpha$ can be found as,

$$d\alpha = \frac{f\ell_o\lambda_{a1}}{C} \tag{13}$$

where

$$\lambda_{a1} = \frac{\sin^2\beta\sin(\alpha)}{2(2\sin^2\beta\cos(\alpha/2) - \sin^2(\alpha/2)\cos\beta\cos(\pi/2n))} \tag{14}$$

Letting $\alpha \approx 120^\circ$, together with Eq. (11), it is simplified as,

$$\lambda_{a1} = \frac{4\sqrt{3} - \sqrt{3}\cos^2\frac{\pi}{2n}}{16 + 2\cos^2\frac{\pi}{2n}} \tag{15}$$

So the energy associated with the bond angle variation $d\alpha$ is,

$$U_{\theta\alpha} = \frac{1}{2}\frac{f^2\ell_o^2\lambda_{a1}^2}{C} \tag{16}$$

Substituting Eq. (13) into Eq. (12), together with Eq. (4), the energy associated with the bond angle variation $d\beta$ can be obtained,

$$U_{\theta\beta} = \frac{1}{2}\frac{f^2\ell_o^2\lambda_{a2}^2}{C} \tag{17}$$

where

$$\lambda_{a2} = \frac{-\sqrt{36 - 9\cos^2\frac{\pi}{2n}}\cos\frac{\pi}{2n}}{32 + 4\cos^2\frac{\pi}{2n}} \tag{18}$$

For an armchair carbon nanotube, the number of the hexagonal carbon ring units along the circumferential direction is 2n. Thus there are 2n bonds a and 4n bonds b in an armchair carbon nanotube along the circumference. Also there are 4n angles α and 8n angles β in an armchair carbon nanotube along the circumference for a hexagonal carbon ring unit composed of two angles α and four angles β. So the total molecular potential energy of an armchair carbon nanotube in hoop direction is,

$$U = \frac{4nf^2}{K} + \frac{4nf^2}{8K} + \frac{2nf^2\ell_o^2\lambda_{a1}^2}{C} + \frac{4nf^2\ell_o^2\lambda_{a2}^2}{C} \tag{19}$$

According to the mechanics of materials, the strain energy of a thin cylinder of thickness t subjected to a pure radial pressure would be,

$$U_b = \frac{1}{2}\int_0^{\ell}\frac{F^2}{E_\theta A}d\ell = \frac{F^2\ell}{2E_\theta A} \tag{20}$$

Based on above hypotheses, we can find that the circumference length of a (n, n) carbon nanotube is $L=2n\,[a+b\cos(\alpha/2)]$; and the hoop force $F=2f$. The sectional area of the nanotube can be written as, $A=[2b\sin(\alpha/2)]\,t=\sqrt{3}\,\ell_o\,t$ (t is the thickness of the nanotube). So the expression of the strain energy of a thin cylinder corresponding to an armchair nanotube is found as,

$$U_b = \frac{2\sqrt{3}nf^2}{E_\theta t} \tag{21}$$

By comparing the total molecular potential energy with the strain energy of a corresponding thin cylinder, the equivalent Young's modulus in the hoop direction of nanotube can be obtained as,

$$E_\theta = \frac{4\sqrt{3}\,KC}{9Ct + 4K\ell_o^2 t(\lambda_{a1} + 2\lambda_{a2}^2)} \tag{22}$$

Eq. (22) shows that Young's modulus of an armchair nanotube in the hoop direction of nanotubes is dependent on parameters λ_{a1} and λ_{a2}. Letting n approaches infinity, then the expressions of Young's modulus of a graphite sheet is given by,

$$E_g = \frac{8\sqrt{3}KC}{18Ct + K\ell_o^2 t} \tag{23}$$

The hoop strain ε_θ and axial strain ε_z of armchair nanotube can be formulated as,

$$\varepsilon_\theta = \frac{d(a + b\cos(\alpha/2))}{a + b\cos(\alpha/2)} \tag{24}$$

$$\varepsilon_z = \frac{d(b\sin(\alpha/2))}{b\sin(\alpha/2)} \tag{25}$$

Substituting the expressions of db and da into the above equations, together with the relations $a = b = \ell_o$ and $\alpha = 120^\circ$, we obtain,

$$\varepsilon_\theta = \frac{9f}{6K\ell_o} + \frac{\sqrt{3}f\ell_o\lambda_{a1}}{6C} \tag{26}$$

$$\varepsilon_z = \frac{f}{2K\ell_o} - \frac{\sqrt{3}f\ell_o\lambda_{a1}}{6C} \tag{27}$$

$$\upsilon_{\theta z} = -\frac{\varepsilon_z}{\varepsilon_\theta} = \frac{\sqrt{3}K\ell_o^2\lambda_{a1} - 3C}{\sqrt{3}K\ell_o^2\lambda_{a1} + 9C} \tag{28}$$

It is interesting to note that both the Poisson's ratio and the surface Young's modulus in hoop direction are exactly same as those in axial direction. This simply indicates that in-plane properties of armchair nanotubes are equivalent, although their molecular structure in axial and hoop directions are different.

B. A zigzag nanotube

For a zigzag nanotube under hoop compression, the nomenclature and force and moment are shown in Fig.

4. The angle between planes OA–OB and OA–OC is given as,

$$\cos\varphi = -\frac{\tan(\alpha/2)}{\tan\beta} \tag{29}$$

And the relationship between α and β yields to equation,

$$\sin(\alpha/2) = \sin(\beta)\cos(\pi/2n) \tag{30}$$

$$d\alpha = 2\frac{\cos\beta}{\cos(\alpha/2)}\cos(\frac{\pi}{2n})d\beta \tag{31}$$

Employing the force equilibrium, the following equation can be obtained,

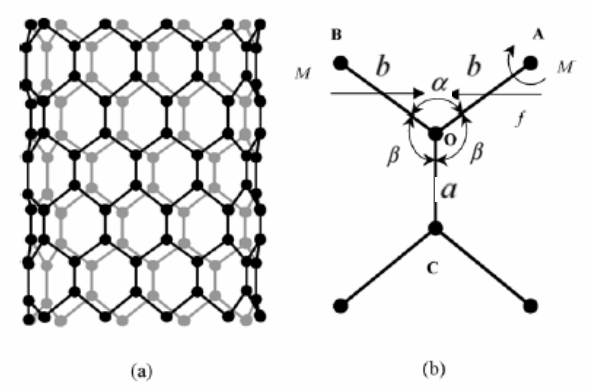

Figure 4. Schematic illustration of (a) a zigzag carbon nanotube, and (b) analytical model for hoop compression.

$$f\sin(\pi-\beta) = kdb, \tag{32}$$

Letting $\beta=120^{\circ}$, then,

$$db = \frac{\sqrt{3}}{2}\frac{f}{K} \tag{33}$$

and from the moment equilibrium, the following equation can be obtained,

$$f\frac{\ell_o}{2}\cos(\pi-\beta) = \quad Cd\beta + Cd\alpha\cos\varphi \tag{34}$$

Similarly, the bond stretching potential energies of a zigzag nanotube would be as,

$$U_{\rho b} = \frac{1}{2}K(db)^2 = \frac{3f^2}{8K} \tag{35}$$

and the potential energies associated with the bond angle variations $d\alpha$ and $d\beta$ are,

$$U_{\theta\alpha} = \frac{f^2\ell_o^2\lambda_{zl}}{2C}, U_{\theta\beta} = \frac{f^2\ell_o^2\lambda_{z2}}{2C} \tag{36}$$

where

$$\lambda_{zl} = \frac{-\sqrt{4-3\cos^2(\frac{\pi}{2n})}\cos(\frac{\pi}{2n})}{8-2\cos^2(\frac{\pi}{2n})} \tag{37}$$

$$\lambda_{z2} = \frac{4-3\cos^2(\frac{\pi}{2n})}{16-4\cos^2(\frac{\pi}{2n})} \tag{38}$$

Thus, based on the structure character of a zigzag nanotube, the total molecular potential energy of a zigzag nanotube can be generated as,

$$U = \frac{6nf^2}{8K} + \frac{f\ell_o^2\lambda_{zl}^2}{C} + \frac{2f\ell_o^2\lambda_{z2}^2}{C} \tag{39}$$

The strain energy of zigzag nanotube under radial pressure simulated with a thin cylinder can be written as,

$$U_b = \frac{\sqrt{3}nf^2}{3E_z t} \tag{40}$$

So the equivalent Young's modulus in the hoop direction of nanotubes of a zigzag nanotube is founded as,

$$E_z = \frac{4\sqrt{3}KC}{9Ct + 12\ell_o^2(\lambda_{zl}^2 + 2\lambda_{z2}^2)} \tag{41}$$

Letting n approaches infinity in λ_{z1} and λ_{z2} we can obtain Young's modulus of a graphite sheet as before (see Eq 23).

The hoop strain ε_θ and axial strain ε_z of the zigzag nanotube can be formulated by using the force equilibrium, as follows,

$$\varepsilon_\theta = \frac{d\left(b\sin(\pi-\beta)\right)}{b\sin(\pi-\beta)} \tag{42}$$

$$\varepsilon_z = \frac{d\left(a+b\cos(\pi-\beta)\right)}{a+b\cos(\pi-\beta)} \tag{43}$$

Substituting the expressions of *db* and *da* into the above equations, together with the relations $a = b = \ell_o$ and $\beta = 120^{\circ}$, one finds,

$$\varepsilon_\theta = \frac{\sqrt{3}}{2}(\frac{f}{K\ell_o} + \frac{2f\ell_o\lambda_{z2}}{3C}) \tag{44}$$

$$\varepsilon_z = \frac{\sqrt{3}}{2}(\frac{f}{3K\ell_o} - \frac{2f\ell_o\lambda_{z2}}{3C}) \tag{45}$$

$$\upsilon_{\theta z} = -\frac{\varepsilon_z}{\varepsilon_\theta} = \frac{2K\ell_o^2\lambda_{z2} - C}{2K\ell_o^2\lambda_{z2} + 3C} \tag{46}$$

Again, both the Poisson's ratio and the surface Young's modulus in hoop direction are exactly same as those in axial direction of zigzag nanotubes. Similar to the armchair nanotubes, in-plane properties in the axial and hoop directions of zigzag nanotubes are equivalent. It should be noted that when one takes $\alpha = \beta = 2\pi/3$ and $n\to\infty$ the above formulations in both

derivations give the properties of the graphene sheet which are also identical in both directions.
From Eqs. (28) and (46), the expression of Poisson's ratio for graphite sheet can be developed as,

$$\nu = \frac{\ell_o^2 K - 6C}{\ell_o^2 K + 18C} \tag{47}$$

C. Shear modulus

Similarly, consider an armchair nanotube subjected to a torsion loading. The analytical model is presented in Fig. 5. When the shear stresses in the two directions are the same, the relationship between f_1 and f_2 is,

$$f_1 = \frac{\sqrt{3}}{3} f_2 \tag{48}$$

The force equilibrium on bond b leads to,

$$f_1 \sin(\alpha/2) + f_2 \cos(\alpha/2) = Kdb \tag{49}$$

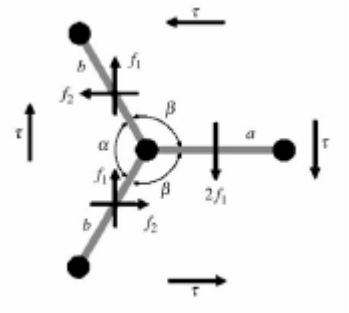

Figure5. Schematic illustration of force distributions of an armchair carbon nanotube.

Letting α=120°, the bond stretching energy can be obtained using Eqs. (49) and (4),

$$U_\rho = \frac{1}{2} K (db)^2 = \frac{f_2^2}{2K} \tag{50}$$

With the moment equilibrium on the right half of bond *b*, one has,

$$f_2 \frac{\ell_o}{2} \sin(\alpha/2) - f_1 \frac{\ell_o}{2} \cos(\alpha/2) = Cd\beta \cos\varphi \tag{51}$$

From Eqs. (51), (10) and (11), the bond angle variation $d\beta$ can be obtained,

$$d\beta = -\frac{f_2 \ell_o \lambda_a}{6C} \tag{52}$$

So the energy associated with the bond angle variation $d\beta$ is equal to,

$$U_\theta = \frac{f_2^2 \ell_o^2 \lambda_a^2}{72C} \tag{53}$$

where

$$\lambda_a = \sqrt{4/\cos^2(\pi/2n) - 1} \tag{54}$$

Thus, the total molecular potential energy of an armchair nanotube can be written as,

$$U = \frac{2Nnf_2^2}{K} + \frac{Nnf_2^2 \ell_o^2 \lambda_a^2}{9C} \tag{55}$$

The torsion strain energy of a thin cylinder corresponding to an armchair nanotube is,

$$U_b = \frac{1}{2} \int_0^\ell \frac{T^2}{G_a J} d\ell = \frac{T^2 \ell}{2 G_a J} \tag{56}$$

where *Ga* is the shear modulus, $T=nf_2R$ is torque and $J=2\pi R^3 t$ is the torsion constant corresponding to thin cylinder. Substituting the expressions of *T*, *J* and *R* in Eq. (56), one can get,

$$U_b = \frac{2\sqrt{3} f_2^2 Nn}{3 G_a t} \tag{57}$$

Based on the equality between Eqs (55) and (57), the equivalent shear modulus of an armchair carbon nanotube is obtained,

$$G_a = \frac{6\sqrt{3}KC}{(18C + K\ell_o^2 \lambda_a^2)t} \tag{58}$$

Letting n approaches infinity in the expression of λ_a; the shear modulus of a graphite sheet is found,

$$G_g = \frac{2\sqrt{3}KC}{(6C + K\ell_o^2)t} \tag{59}$$

Fig. 6. shows the analytical model of a zigzag nanotube subjected to torsion. The equilibrium equations of the force and moment are given by,

$$f1 \cos(\pi - \beta) + f_2 \sin(\pi - \beta) = Kdb \tag{60}$$

$$2f_2 \frac{\ell_o}{2} = 2Cd\beta \cos\varphi \tag{61}$$

and

$$f_1 = \sqrt{3} f_2 \tag{62}$$

Similarly, the bond stretching potential energy and the potential energy associated with the bond angle variation $d\beta$ of a zigzag nanotube can be found as,

$$U_\rho = \frac{3f^2}{2K} \tag{63}$$

$$U_\theta = \frac{3f^2 \ell_o^2 \lambda_z^2}{8C} \tag{64}$$

where

$$\lambda_z = \sqrt{4/3\cos^2(\pi/2n) - 1} \tag{65}$$

So, the total molecular potential energy of a zigzag carbon nanotube can de written as,

$$U = \frac{3Nnf^2}{K} + \frac{3Nnf^2 \ell_o^2 \lambda_z^2}{2C} \tag{66}$$

And the torsion strain energy of a thin cylinder corresponding to a zigzag carbon nanotube would be,

$$U_b = \frac{\sqrt{3} f^2 Nn}{Gt} \qquad (67)$$

Thus, the expression for the shear modulus of an armchair carbon nanotube is obtained as follows,

$$G = \frac{2\sqrt{3}KC}{6Ct + 3K\ell_0^2\lambda_z^2 t} \qquad (68)$$

Using Eq. (68), the shear modulus of a graphite sheet can be derived. (See Eq 59).

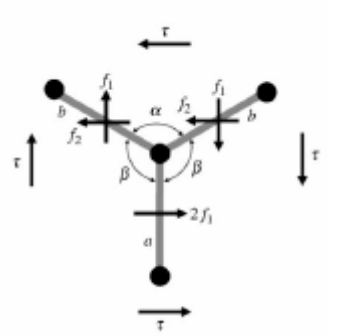

Figure6. Schematic illustration of force distributions of a zigzag carbon.nanotube.

IV. RESULTS AND DISCUSSIONS

Noting the relations obtained for Young's and shear modulus, it can be seen that the tube thickness *t* is an important parameter in determining the mechanical properties of single-walled carbon nanotubes. However, there is no agreement regarding thickness estimation. Some researchers assumed that *t* is equal to 0.34 nm, which is the interlayer spacing of graphite. Therefore, the equivalent Young's modulus was determined based on this value. But, different values of the tube thickness, such as 0.066nm, 0.65nm and 0.0617 nm, has been suggested as well.

In this study, the parameter are selected as, K =742 nN/nm, C =1.42 nN.nm/rad^2 and the experimental value of Young's modulus graphite is set to 1.06TPa. then the tube thickness, *t* = 0.34nm can be obtained from Eq. (23). Using this value of *t*, the predicted graphite shear modulus according to the present study is resulted as 0.457 TPa which shows good agreement with the experimental value 0.47 TPa reported in Ref. [9]. Also, the graphite Poisson's ratio is estimated 0.159 which is a reasonable value too, so *t* = 0.34nm is used as the tube thickness in the following analysis.

Fig. 7. shows the variation of the Young's modulus in hoop direction with nanotube diameter that is exactly the same as Young modulus in axial direction [10]. It can be seen that the Young's modulus for both armchair and zigzag nanotubes increase with increasing tube diameter. For a given tube diameter, Young's modulus of armchair nanotubes is slightly larger than that of zigzag nanotubes. The variation of CNTs shear modulus shows the same trend as presented in Fig. 8. Although in contrast to modulus of elasticity, zigzag nanotubes have slightly larger shear modulus in comparison to armchair modulus. In Figs. 9 and 10 variation of Young's and Shear modulus for two types of CNTs as a function of the thickness are presented, respectively. It is obvious that both armchair (12, 12) and zigzag (21, 0) SWCNTs exhibit the same mechanical properties in the range of thickness considered. Also, it is seen that Young's and Shear modulus decrease significantly as the thickness of the CNT increases. Fig. 11. shows distribution of Poisson's ratio as a function of tube diameter. It is clear that for both armchair and zigzag nanotubes Poisson's ratio decrease monotonically with increasing the diameter. Furthermore zigzag nanotubes exhibit a larger Poisson's ratio at a known diameter comparison to armchair.

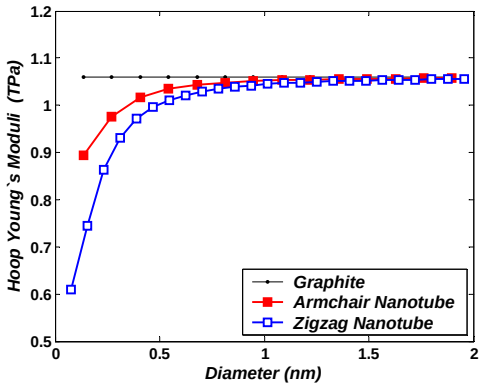

Figure7. The Young's modulus in hoop direction (E_θ)

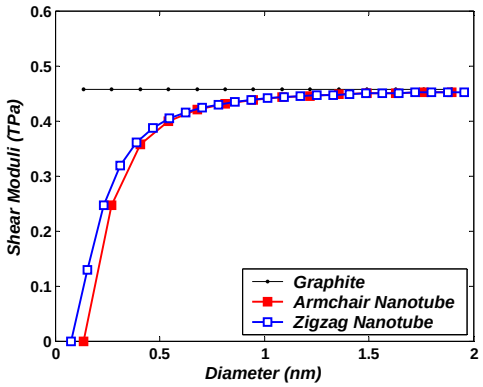

Figure8. The variation of shear modulus

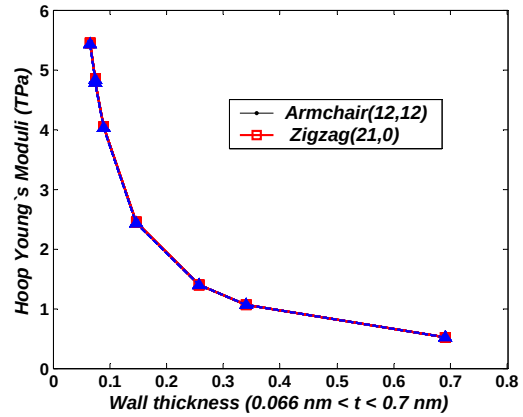

Figure9. Young's modulus in hoop direction (E_θ) of (12, 12) and (21, 0) carbon nanotubes versus thickness.

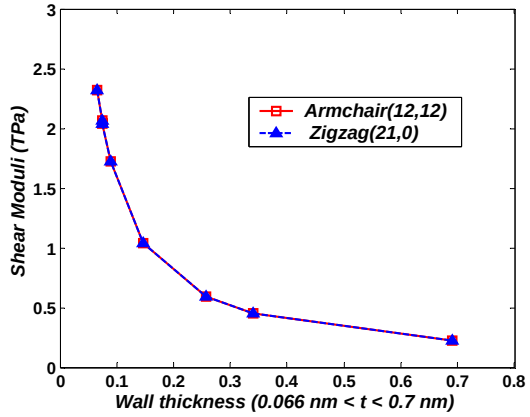

Figure10. Shear modulus of (12, 12) and (21, 0) carbon nanotubes versus thickness.

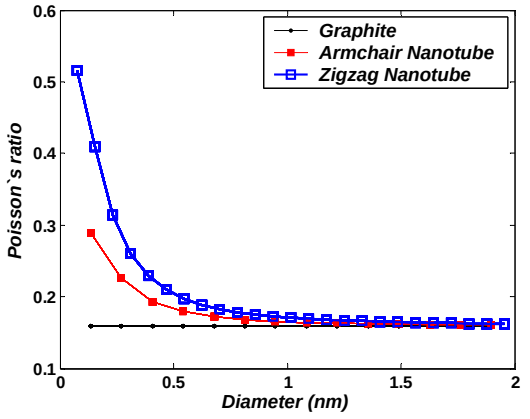

Figure11. The variation of Poisson ratio ($\nu_{\theta z}$).

From Figs. 7–11. the results indicate that the in-plane properties of nanotubes in axial and hoop directions are equivalent and sensitive to tube diameter at small diameter ranges and wall-thickness. It can be clearly observed that for carbon nanotubes with smaller diameter, for example, less than 1.0 nm, Young's modulus in hoop direction, shear modulus and Poisson's ratio in hoop direction exhibit a strong dependence on the diameter. However for those with larger diameter, this dependency becomes very weak. The reason for this phenomenon is that a carbon nanotube with smaller diameter has a larger curvature, which results in a more significant distortion of C–C bonds. As the nanotube diameter increases, the effect of curvature diminishes gradually, and all of Young's modulus, shear modulus and Poisson's ratio approach to the values of graphite sheet as predicted by the present model and as well as those reported in literature [5-10,12].

Fig. 12. shows the comparison between Young's modulus in hoop direction predicted from the present model with the existing results [12]. It can be seen that although there are some differences at the plateau level, which can be generated from the assumed Young's modulus of graphite sheet, in different models, [5-10,12], but the general trends of the solutions are in good agreement.

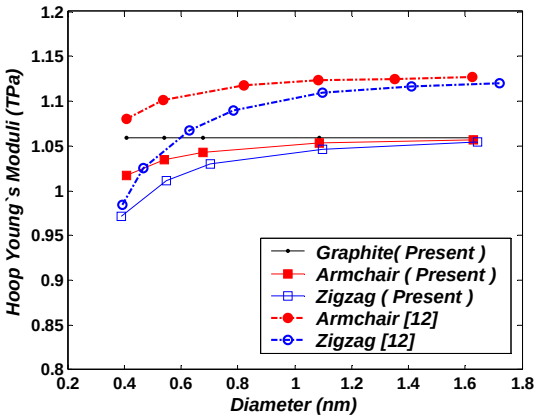

Figure12. Young's moduli in hoop direction (E_θ) of carbon nanotubes versus tube diameter.

Fig. 13. presents the comparison among the Shear modulus resulted from the present model and existed solutions [9]. Again reasonable agreement among the solution is demonstrated. The predicted graphite shear modulus in the present study is 0.457 TPa, which is close to the theoretical values of 0.47 TPa reported by Xiao et al. [9].

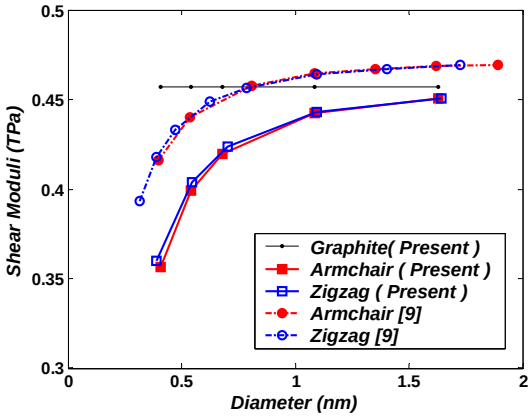

Figure13. Shear moduli of carbon nanotubes versus tube diameter.

A comparison of Poisson's ratio predicted by the presented solutions with those of Ref. [12] is shown in Fig. 14. for two types of nanotubes. Good agreement is achieved as before. Although many investigations for Poisson's ratio of nanotubes have been conducted, there is no unique opinion that is widely accepted. But the present results agree well with the theoretical results provided by other modeling techniques.

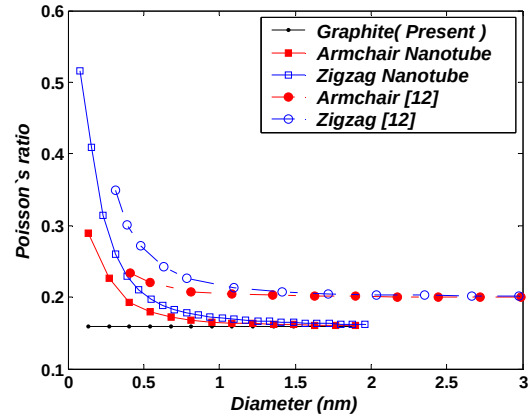

Figure14. Poisson's ratios ($\nu_{\theta z}$) of carbon nanotubes versus tube diameter.

Lastly, the stress-strain curve for the armchair SWCNT predicted. It can be seen that the Young's modulus for armchair nanotubes increase with increasing tube diameter, also it is obvious that the Young's modulus is identical to the tangent of stress-strain curve's angle. So, this result is depicted in Fig. 15. As can be seen in Fig. 15, the tensile strength of 126.2 GPa and failure strain of 23.1% are predicted for (12, 12) armchair nanotube. Again these predictions agree well with the numerical results.

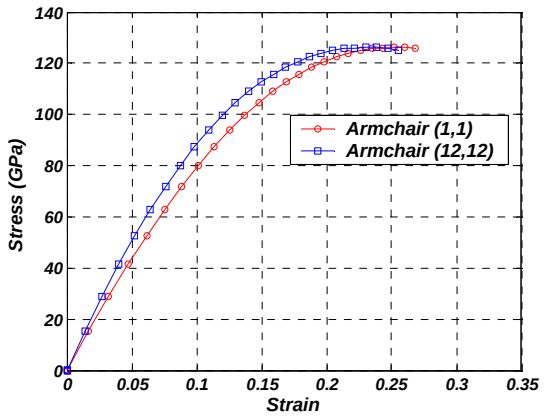

Figure15. stress–strain curves for armchair nanotubes.

REFERENCES

[1] Iijima S, "Helical microtubules of graphitics carbon", Nature, London, 1991, 354:56–8.

[2] Sumio Iijima, "Carbon nanotubes: past, present, and future", Physica B, 2002 , 323 1–5.

[3] Zhang, P., Huang, Y.,Gao, H., Hwang, K.C. "Fracture nucleation in single-wall carbon nanotubes under tension: continuum analysis incorporating interatomic potentials", J.Appl.Mech ,2002a,Trans.ASME 69,454–458.

[4] Zhang, P., Huang, Y., Geubelle, P.H., Klein, P., Hwang, K.C., "The elastic modulus of single-wall carbon nanotubes: continuum analysis incorporating interatomic potentials" Int.J.Solids Struct ,2002b,39,3893–3906.

[5] C. Li, T.-W. Chou, "A structural mechanics approach for the analysis of carbon nanotubes", International Journal of Solids and Structures 40, 2005, 2487–2499.

[6] K.I.Tsepres, P.Papanikos, "Finite element modeling of single-walled carbon nanotubes", CompositesPartB36, 2005, 468–477.

[7] G.I. Giannopoulos, P.A. Kakavas, N.K.Anifantis , "Evaluation of the effective mechanical properties of single walled carbon nanotubes using a spring based finite element approach", Computational Materials Science,2007.

[8] T.Changa, H. Gao, "Size-dependent elastic properties of a single-walled carbon nanotube via a molecular mechanics model", Journal of the Mechanics and Physics of Solids 51 ,2003,1059 – 1074.

[9] J.R. Xiao, B.A. Gama, J.W. Gillespie Jr., "An analytical molecular structural mechanics model for the mechanical properties of carbon nanotubes", International Journal of Solids and Structures 42, 2005, 3075–3092.

[10] Y.Wu, X.Zhang, A.Y.T. Leung, W.Zhong, "An energy-equivalent model on studying the mechanical properties of single-walled carbon nanotubes", Thin-Walled Structures 44, 2006, 667–676.

[11] M.ENDO, SUMIO.IIJIMA,M.S. DRESSELHAUS, *CARBON NANOTUBES*, *Elsevier Science*, Great Britain , 1996

[12] J.R. Xiao , S.L. Lopatnikov , B.A. Gama, J.W. Gillespie Jr. "Nanomechanics on the deformation of single- and multi-walled carbon nanotubes under radial pressure", Materials Science and Engineering A 416 ,2006, 192–2.